54. Chen J, Gu G (2000) Control Oriented System Identification, An $\mathcal{H}_\infty$ Approach. Wiley, New York
55. Ljung L, Soderstrom T (1983) Theory and Practice of Recursive Identification. MIT Press, Cambridge
56. Ljung L (1996) Development of system identification. In: IFAC Congress, vol G, pp 141–146
57. Milanese M, Vicino A (1991) Optimal estimation theory for dynamic systems with set membership uncertainty: an overview. Automatica 27:997–1009
58. Helmicki AJ, Jacobson CA, Nett CN (1989) $\mathcal{H}_\infty$ identification of stable lsi systems: A scheme with direct application to controller design. In: American Contol Conference, Pittsburgh pp 1428–1434
59. Gu G, Khargonekar PP, Li Y (1992) Robust convergence of twostage nonlinear algorithms for system identification. Syst Control Lett 18:253–263
60. Chen J, Nett C, Fan M (1995) Worst-case system identification in $\mathcal{H}_\infty$: Validation of a Priori information, essentially optimal algorithms and error bounds. IEEE Trans Autom Control 40(7):1260–1265
61. Foias C, Frazho AE (1990) The commutant lifting approach to interpolation problems, Operator theory: Advances and Applications, vol 44. Birkhäuser, Basel
62. Ball J, Gohberg I, Rodman L (1990) Interpolation of Rational Matrix Functions, Operator Theory: Advances and Applications, vol 45. Birkhäuser, Basel

Books and Reviews

Chen J, Gu G (2000) Control Oriented System Identification, An $\mathcal{H}_\infty$ Approach. Wiley, New York. An excellent reference book with an in depth coverage of Robust Identification and the associated mathematical background in Interpolation Theory

Fisher RB, CV-Online: The Evolving, Distributed, Non-Proprietary, On-Line Compendium of Computer Vision, Online Book, 2007 Provides a very complete online, evolving hypertext summary on central topics in computer vision, including motion and tracking

Forsyth DA, Ponce J (2003) Computer Vision: A Modern Approach, Prentice Hall, Prentice Hall, Upper Saddle River. A textbook covering the fundamentals of computer vision. Chapter 4 includes an introduction to the problem of tracking using linear models

Ma Y, Soatto S, Kosecka J, J Sastry, Sastry SS (2005) An Invitation to 3-D Vision, From Images to Geometric Models. Springer, Berlin. Chapter 12 is dedicated to the topic of visual feedback including applications to autonomous navigation

Medioni G, Kang SB (2005) Emerging Topics is Computer Vision, Prentice Hall, Prentice Hall, Upper Saddle River. Chapter 11 provides a tutorial on the open source computer vision library OpenCV

Paoletti S, Juloski A, Ferrari-Trecate G, Vidal R (2007) Identification of Hybrid Systems: A Tutorial. Eur J Control 13(2–3). A survey paper covering the fundamentals of identification of piecewise affine models

Sánchez Peña R, Sznaier M (1998) Robust Systems Theory and Applications. Wiley, New York. Chapter 10 of this textbook provides a good introduction to the field of Robust Identification. In: addition, the Appendices provide a summary of several key results in Linear Systems Theory

Sznaier M, Camps O (2007) Systems Theoretic Methods in Computer Vision and Image Processing. J Soc Inst Contr Eng. (SICE) Special Issue on Control Theoretic Principles in Emerging Technologies 46:p 206, A survey paper that covers the use of systems theoretic tools to solve multiple problems arising in the context of dynamic vision and image processing, e. g. tracking, motion segmentation, structure from motion, activity recognition, texture modeling and recognition, static and dynamic inpainting, etc

Movement Coordination

Armin Fuchs[1,2], James A. S. Kelso[1]
[1] Center for Complex Systems & Brain Sciences, Florida Atlantic University, Boca Raton, USA
[2] Department of Physics, Florida Atlantic University, Boca Raton, USA

Article Outline

Glossary

Control parameter A parameter of internal or external origin that when manipulated controls the system in a nonspecific fashion and is capable of inducing changes in the system's behavior. These changes may be a smooth function of the control parameter, or abrupt at certain critical values. The latter, also referred to as phase transitions, are of main interest here as they only occur in nonlinear systems and are accompanied by phenomena like critical slowing down and fluctuation enhancement that can be probed for experimentally.

Haken–Kelso–Bunz (HKB) model First published in 1985, the HKB model is the best known and probably most extensively tested quantitative model in human movement behavior. In its original form it describes the dynamics of the relative phase between two oscillating fingers or limbs under frequency scaling. The HKB model can be derived from coupled nonlinear os-

cillators and has been successfully extended in various ways, for instance, to situations where different limbs like an arm and a leg, a single limb and a metronome, or even two different people are involved.

Order parameter Order parameters are quantities that allow for a usually low-dimensional description of the dynamical behavior of a high-dimensional system on a macroscopic level. These quantities change their values abruptly when a system undergoes a phase transition. For example, density is an order parameter in the ice to water, or water to vapor transitions. In movement coordination the most-studied order parameter is relative phase, i. e. the difference in the phases between two or more oscillating entities.

Phase transition The best-known phase transitions are the changes from a solid to a fluid phase like ice to water, or from fluid to gas like water to vapor. These transitions are called first-order phase transitions as they involve latent heat, which means that a certain amount of energy has to be put into the system at the transition point that does not cause an increase in temperature. For the second-order phase transitions there is no latent heat involved. An example from physics is heating a magnet above its Curie temperature at which point it switches from a magnetic to a nonmagnetic state. The qualitative changes that are observed in many nonlinear dynamical systems when a parameter exceeds a certain threshold are also such second-order phase transitions.

Definition of the Subject

Movement Coordination is present all the time in daily life but tends to be taken for granted when it works. One might say it is quite an arcane subject also for science. This changes drastically when some pieces of the locomotor system are not functioning properly because of injury, disease or age. In most cases it is only then that people become aware of the complex mechanisms that must be in place to control and coordinate the hundreds of muscles and joints in the body of humans or animals to allow for maintaining balance while maneuvering through rough terrains, for example. No robot performance comes even close in such a task.

Although these issues have been around for a long time it was only during the last quarter century that scientists developed quantitative models for movement coordination based on the theory of nonlinear dynamical systems. Coordination dynamics, as the field is now called, has become arguably the most developed and best tested quantitative theory in the life sciences.

More importantly, even though this theory was originally developed for modeling of bimanual finger movements, it has turned out to be universal in the sense that it is also valid to describe the coordination patterns observed between different limbs, like an arm and a leg, different joints within a single limb, like the wrist and elbow, and even between different people that perform movements while watching each other.

Introduction

According to a dictionary definition: *Coordination* is the act of coordinating, making different people or things work together for a goal or effect.

When we think about *movement coordination* the "things" we make work together can be quite different like our legs for walking, fingers for playing the piano, mouth, tongue and lips for articulating speech, body expressions and the interplay between bodies in dancing and ballet, tactics and timing between players in team sports and so on, not to forget other advanced skill activities like skiing or golfing.

All these actions have one thing in common: they look extremely easy if performed by people who have learned and practiced these skills, and they are incredibly difficult for novices and beginners. Slight differences might exist regarding how these difficulties are perceived, for instance when asked whether they can play golf some people may say: "I don't know, let me try", and they expect to out-drive Tiger Woods right away; there are very few individuals with a similar attitude toward playing the piano.

The physics of golf as far as the ball and the club is concerned is almost trivial: hit the ball with the highest possible velocity with the club face square at impact, and it will go straight and far. The more tricky question is how to achieve this goal with a body that consists of hundreds of different muscles, tendons and joints, and, importantly, their sensory support in joint, skin and muscle receptors (proprioception), in short, hundreds of degrees of freedom. How do these individual elements work together, how are they coordinated? Notice, the question is not how do *we* coordinate them? None of the skills mentioned above can be performed by consciously controlling all the body parts involved. Conscious thinking sometimes seems to do more harm than good. So how do they/we do it? For some time many scientists sought the answer to this question in what is called *motor programs* or, more recently, *internal models*. The basic idea is straightforward: when a skill is learned it is somehow stored in the brain like a program in a computer and simply can be called and executed when needed. Additional learning or train-

ing leads to skill improvement, interpreted as refinements in the program. As intuitive as this sounds and even if one simply ignores all the unresolved issues like how such programs gain the necessary flexibility or in what form they might be stored in the first place, there are even deeper reasons and arguments suggesting that humans (or animals for that matter) don't work like that. One of the most striking of these arguments is known as motor equivalence: everybody who has learned to write with one of their hands can immediately write with the foot as well. This writing may not look too neat, but it will certainly be readable and represents the transfer of a quite complex and difficult movement from one end-effector (the hand) to another (the foot) that is controlled by a completely different set of muscles and joints. Different degrees of freedom and redundancy in the joints can still produce the same output (the letters) immediately, i. e. without any practice.

For the study of movement coordination a most important entry point is to look at situations where the movement or coordination pattern changes abruptly. An example might be the well-known gait switches from walk to trot to gallop that horses perform. It turns out, however, that switching among patterns of coordination is a ubiquitous phenomenon in human limb movements. As will be described in detail, such switching has been used to probe human movement coordination in quantitative experiments.

It is the aim of this article to describe an approach to a quantitative modeling of human movements, called coordination dynamics, that deals with quantities that are accessible from experiments and makes predictions that can and have been tested. The intent is to show that coordination dynamics represents a theory allowing for quantitative predictions of phenomena in a way that is unprecedented in the life sciences. In parallel with the rapid development of noninvasive brain imaging techniques, coordination dynamics has even pointed to new ways for the study of brain functioning.

The Basic Law of Coordination: Relative Phase

The basic experiment, introduced by one of us [27,28], that gave birth to coordination dynamics, the theory underlying the coordination of movements, is easily demonstrated and has become a classroom exercise for generations of students: if a subject is moving the two index fingers in so-called anti-phase, i. e. one finger is flexing while the other is extending, and then the movement rate is increased, there is a critical rate where the subject switches spontaneously from the anti-phase movement to in-phase, i. e. both fingers are now flexing and extending at the same time. On the other hand, if the subject starts at a high or low rate with an in-phase movement and the rate is slowed down or sped up, no such transition occurs.

These experimental findings can be translated or mapped into the language of dynamical systems theory as follows [19]:

- At low movement rates the system has two stable attractors, one representing anti-phase and one for in-phase – in short: the system is bistable;
- When the movement rate reaches a critical value, the anti-phase attractor disappears and the only possible stable movement pattern remaining is in-phase;
- There is strong hysteresis: when the system is performing in-phase and the movement rate is decreased from a high value, the anti-phase attractor may reappear but the system does not switch to it.

In order to make use of dynamical systems theory for a quantitative description of the transitions in coordinated movements, one needs to establish a measure that allows for a formulation of a dynamical system that captures these experimental observations and can serve as a phenomenological model. Essentially, the finger movements represent oscillations (as will be discussed in more detail in Subsect. "Oscillators for Limb Movements") each of which is described by an amplitude r and a phase $\varphi(t)$. For the easiest case of harmonic oscillations the amplitude r does not depend on time and the phase increases linearly with time at a constant rate ω, called the angular velocity, leading to $\varphi(t) = \omega t$. Two oscillators are said to be in the in-phase mode if the two phases are the same, or $\varphi_1(t) - \varphi_2(t) = 0$, and in anti-phase if the difference between their two phases is 180° or π radians. Therefore, the quantity that is most commonly used to model the experimental findings in movement coordination is the phase difference or *relative phase*

$$\phi(t) = \varphi_1(t) - \varphi_2(t) = \begin{cases} \phi(t) = 0 & \text{for in-phase} \\ \phi(t) = \pi & \text{for anti-phase} . \end{cases} \tag{1}$$

The minimal dynamical system for the relative phase that is consistent with observations is known as the Haken–Kelso–Bunz (or HKB) model and was first published in a seminal paper in 1985 [19]

$$\dot{\phi} = -a \sin\phi - 2b \sin 2\phi \quad \text{with} \quad a, b \geq 0 . \tag{2}$$

As is the case for all one-dimensional first order differential equations, (2) can be derived from a potential function

$$\dot{\phi} = -\frac{\mathrm{d}V(\phi)}{\mathrm{d}\phi} \quad \text{with} \quad V(\phi) = -a\cos\phi - b\cos 2\phi . \tag{3}$$

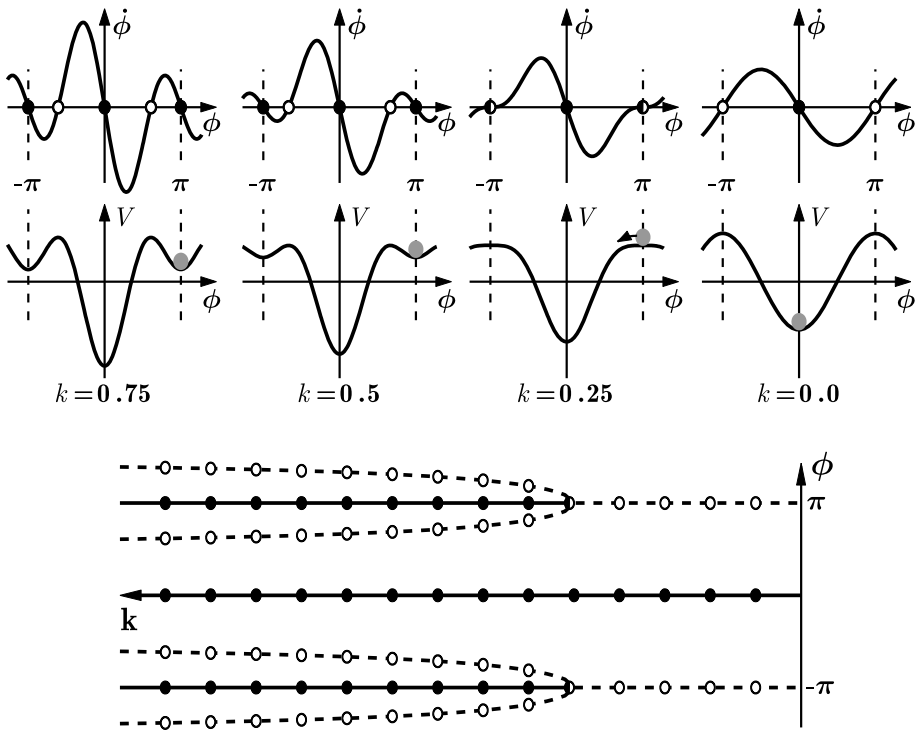

Movement Coordination, Figure 1
Dynamics of the HKB model at the coordinative, relative phase (ϕ) level as a function of the control parameter $k = \frac{b}{a}$. *Top row*: Phase space plots $\dot{\phi}$ as a function of ϕ. *Middle*: Landscapes of the potential function $V(\phi)$. *Bottom*: Bifurcation diagram, where *solid lines* with *filled circles* correspond to stable fixed points (attractors) and *dashed lines* with *open circles* denote repellers. Note that k increases from right ($k = 0$) to left ($k = 0.75$)

One of the two parameters a and b that appear in (2) and (3) can be eliminated by introducing a new time scale $\tau = \alpha t$, a procedure known as scaling and commonly used within the theory of nonlinear differential equations, leading to

$$\begin{aligned} \dot{\phi}(t) = \frac{\mathrm{d}\phi(t)}{\mathrm{d}t} \quad &\rightarrow \quad \frac{\mathrm{d}\phi\left(\frac{\tau}{\alpha}\right)}{\mathrm{d}\frac{\tau}{\alpha}} \\ &= -a \sin\phi\left(\frac{\tau}{\alpha}\right) - 2b \sin 2\phi\left(\frac{\tau}{\alpha}\right) \qquad (4) \\ \alpha \frac{\mathrm{d}\tilde{\phi}(\tau)}{\mathrm{d}\tau} &= -a \sin\tilde{\phi}(\tau) - 2b \sin 2\tilde{\phi}(\tau) \end{aligned}$$

where $\tilde{\phi}$ has the same shape as ϕ, it is just changing on a slower or faster time scale depending on whether α is bigger or smaller than 1. After dividing by α and letting the so far undetermined $\alpha = a$ (4) becomes

$$\frac{\mathrm{d}\tilde{\phi}}{\mathrm{d}\tau} = -\underbrace{\frac{a}{\alpha}}_{=1} \sin\tilde{\phi} - 2\underbrace{\frac{b}{\alpha}}_{=k} \sin 2\tilde{\phi}\,. \qquad (5)$$

Finally, by dropping the tilde ˜ (2) and (3) can be written with only one parameter $k = \frac{b}{a}$ in the form

$$\begin{aligned} \dot{\phi} &= -\sin\phi - 2k \sin 2\phi \\ &= -\frac{\mathrm{d}V(\phi)}{\mathrm{d}\phi} \quad \text{with} \quad V(\phi) = -\cos\phi - k\cos 2\phi\,. \qquad (6) \end{aligned}$$

The dynamical properties of the HKB model's *collective* or *coordinative* level of description are visualized in Fig. 1 with plots of the phase space ($\dot{\phi}$ as a function of ϕ) in the top row, the potential landscapes $V(\phi)$ in the second row and the bifurcation diagram at the bottom. The control parameter k, as shown, is the ratio between b and a, $k = \frac{b}{a}$, which is inversely related to the movement rate: a large value of k corresponds to a slow rate, whereas k close to zero indicates that the movement rate is high.

In the phase space plots (Fig. 1 top row) for $k = 0.75$ and $k = 0.5$ there exist two stable fixed points at $\phi = 0$ and $\phi = \pi$ where the function crosses the horizontal axis with a negative slope, marked by solid circles (the fixed point at $-\pi$ is the same as the point at π as the function is 2π-periodic). These attractors are separated by repellers,

zero crossings with a positive slope and marked by open circles. For the movement rates corresponding to these two values of k the model suggests that both anti-phase and in-phase movements are stable. When the rate is increased, corresponding to a decrease in the control parameter k down to the critical point at $k_c = 0.25$ the former stable fixed point at $\phi = \pi$ collides with the unstable fixed point and becomes neutrally stable indicated by a half-filled circle. Beyond k_c, i. e. for faster rates and smaller values of k the anti-phase movement is unstable and the only remaining stable coordination pattern is in-phase.

The potential functions, shown in the second row in Fig. 1, contain the same information as the phase space portraits as they are just a different representation of the dynamics. However, the strong hysteresis is more intuitive in the potential landscape than in phase space, and can best be seen through an experiment that starts out with slow movements in anti-phase (indicated by the gray ball in the minimum of the potential at $\phi = \pi$) and increasing rate. After passing the critical value $k_c = 0.25$ the slightest perturbation will put the ball on the downhill slope and initiate a switch to in-phase. If the movement is now slowed down again, going from right to left in the plots, even though the minimum at $\phi = \pi$ reappears, the ball cannot jump up and occupy it but will stay in the deep minimum at $\phi = 0$, a phenomenom known as hysteresis.

Finally, a bifurcation diagram is shown at the bottom of Fig. 1, where the locations of stable fixed points for the relative phase ϕ are plotted as solid lines with solid circles and unstable fixed points as dashed lines with open circles. Around $k_c = 0.25$ the system undergoes a subcritical pitchfork bifurcation. Note that the control parameter k in this plot increases from right to left.

Evidently, the dynamical system represented by (2) is capable of reproducing the basic experimental findings listed above. From the viewpoint of theory, this is simply one of the preliminaries for a model that have to be fulfilled. In general, any model that only reproduces what is built into it is not of much value. More important are crucial experimental tests of the consequences and additional phenomena that are predicted when the model is worked through. Several such consequences and predictions will be described in detail in the following sections. It is only after such theoretical and experimental scrutiny that the HKB model has come to qualify as an elementary law of movement coordination.

Stability: Perturbations and Fluctuations

Random fluctuations, or noise for short, exist in all systems that dissipate energy. In fact, there exists a famous theorem that goes back to Einstein, known as the dissipation-fluctuation theorem, which states that the amount of random fluctuations in a system is proportional to its dissipation of energy. There are effects from random noise on the dynamics of relative phase that can be predicted from theory both qualitatively and quantitatively, allowing for the HKB model's coordination level to be tested experimentally. Later the individual component level will be discussed.

An essential difference between the dynamical systems approach to movement coordination and the motor program or internal model hypotheses is most distinct in regions where the coordination pattern undergoes a spontaneous qualitative change as in the switch from anti-phase to in-phase in Kelso's experiment. From the latter point of view, these switches simply happen, very much like in the automatic transmission of a car: whenever certain criteria are fulfilled, the transmission switches from one gear to another. It is easy to imagine a similar mechanism to be at work and in control of the transitions in movements: as soon as a certain rate is exceeded, the anti-phase program is somehow replaced by the in-phase module, which is about all we can say regarding the mechanism of switching. On the other hand, by taking dynamic systems theory seriously, one can predict and test phenomena accompanying second-order phase transitions. Three of these phenomena, namely, critical slowing down, enhancement of fluctuations and critical fluctuations will be discussed here in detail.

For a quantitative treatment it is advantageous to expand $\dot{\phi}$ and $V(\phi)$ in (6) into Taylor series around the fixed point $\phi = \pi$ and truncate them after the linear and quadratic terms, respectively

$$\begin{aligned}
\dot{\phi} &= -\sin\phi - 2k\sin 2\phi \\
&= -\{-(\phi-\pi) + \ldots\} - 2k\{2(\phi-\pi) + \ldots\} \\
&\approx (1-4k)(\phi-\pi) \\
V(\phi) &= -\cos\phi - k\cos 2\phi \\
&= -\{-1 + (\phi-\pi)^2 + \ldots\} \\
&\quad - k\{1 - 4(\phi-\pi)^2 + \ldots\} \\
&\approx 1 - k - (1-4k)(\phi-\pi)^2 \,.
\end{aligned} \tag{7}$$

A typical situation that occurs when a system approaches and passes through a transition point is shown in Fig. 2. In the top row the potential function for $\phi \geq 0$ is plotted (dashed line) together with its expansion around the fixed point $\phi = \pi$ (solid). The bottom row consists of plots of time series showing how the fixed point is or is not approached when the system is initially at $\phi = \pi + \Delta$. The phenomena accompanying second-order phase tran-

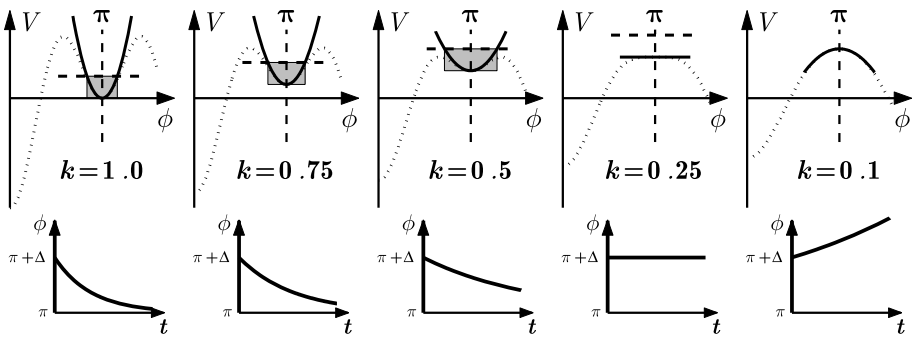

Movement Coordination, Figure 2
Hallmarks of a system that approaches a transition point: enhancement of fluctuations, indicated by the increasing size of the *shaded area*; critical slowing down shown by the time it takes for the system to recover from a perturbation (*bottom*); critical fluctuations occur where the top of the shaded area is higher than the closest maximum in the potential, initiating a switch even though the system is still stable

sitions in a system that contains random fluctuations can be best described by Fig. 2.

Critical slowing down corresponds to the time it takes the system to recover from a small perturbation Δ. In the vicinity of the fixed point the dynamics can be described by the linearization of the nonlinear equation around the fixed point (7). Such a linear equation can be readily solved leading to

$$\phi(t) = \pi + \Delta e^{(1-4k)t} .$$

As long as k is larger than its critical value $k_c = 0.25$ the exponent is negative and a perturbation will decay exponentially in time. However, as the system approaches the transition point, this decay will take longer and longer as shown in the bottom row in Fig. 2. At the critical parameter $k = 0.25$ the system will no longer return to the former stable fixed point and beyond that value it will even move away from it. In the latter parameter region the linear approximation is no longer valid. Critical slowing down can be and has been tested experimentally by perturbing a coordination state and measuring the relaxation constant as a function of movement rate prior to the transition. The experimental findings [31,44,45] are in remarkable agreement with the theoretical predictions of coordination dynamics [43].

Enhancement of fluctuations is to some extent the stochastic analog to critical slowing down. The random fluctuations that exist in all dissipative systems are a stochastic force that kicks the system away from the minimum and (on average) up to a certain elevation in the potential landscape, indicated by the shaded areas in Fig. 2. For large values of k the horizontal extent of this area is small but becomes larger and larger when the transition point is approached. Assuming that the strength of the random force does not change with the control parameter, the standard deviation of the relative phase is a direct measure of this enhancement of fluctuations and will be increasing when the control parameter is moving towards its critical value. Again experimental tests are in detailed agreement with the stochastic version of the HKB model [30,43,44].

Critical fluctuations can induce transitions even when the critical value of the control parameter has not been reached. As before, random forces will kick the system around the potential minimum and up to (on average) a certain elevation. If this height is larger than the hump it has to cross, as is the case illustrated in Fig. 2 for $k = 0.5$, a transition will occur, even though the fixed point is still classified as stable. In excellent agreement with theory, such critical fluctuations were observed in the original experiments by Kelso and colleagues [30] and have been found in a number of related experimental systems [31,42].

All these hallmarks point to the conclusion that transitions in movement coordination are not simply a switching of gears but take place in a well defined way via the instability of a former stable coordination state. Such phenomena are also observed in systems in physics and other disciplines where in situations far from thermal equilibrium macroscopic patterns emerge or change, a process termed self-organization. A general theory of self-organizing systems, called synergetics [17,18], was formulated by Hermann Haken in the early 1970s.

The Oscillator Level

The foregoing description and analysis of bimanual movement coordination takes place on the coordinative or collective level of relative phase. Looking at an actual experiment, there are two fingers moving back and forth and one may ask whether it is possible to find a model on the level of the oscillatory components from which the dynamics of the relative phase can then be derived. The challenge for such an endeavor is at least twofold: first, one needs a dynamical system that accurately describes the movements of the individual oscillatory components (the fingers). Second, one must find a coupling function for these components that leads to the correct relation for the relative phase (2).

Oscillators for Limb Movements

In terms of oscillators there is quite a variety to choose from as most second order systems of the form

$$\ddot{x} + \gamma\dot{x} + \omega^2 x + N(x, \dot{x}) = 0 \tag{8}$$

are potential candidates. Here ω is the angular frequency, γ the linear damping constant and $N(x, \dot{x})$ is a function containing nonlinear terms in x and $\dot{x}$.

Best known and most widely used are the harmonic oscillators, where $N(x, \dot{x}) = 0$, in particular for the case without damping $\gamma = 0$. In the search for a model to describe human limb movements, however, harmonic oscillators are not well suited, because they do not have stable limit cycles. The phase space portrait of an harmonic oscillator is a circle (or ellipse), but only if it is not perturbed. If such a system is slightly kicked off the trajectory it is moving on, it will not return to its original circle but continue to move on a different orbit. In contrast, it is well known that if a rhythmic human limb movement is perturbed, this perturbation decreases exponentially in time and the movement returns to its original trajectory, a stable limit cycle, which is an object that exists only for nonlinear oscillators [25,26].

Obviously, the amount of possible nonlinear terms to choose from is infinite and at first sight, the task to find the appropriate ones is like looking for a needle in a haystack. However, there are powerful arguments that can be made from both theoretical reasoning and experimental findings that restrict the nonlinearities, as we shall see, to only two. First, we assume that the function $N(x, \dot{x})$ takes the form of a polynomial in x and $\dot{x}$ and that this polynomial is of the lowest possible order. So the first choice would be to assume that N is quadratic in x and $\dot{x}$ leading to an oscillator of the form

$$\ddot{x} + \gamma\dot{x} + \omega^2 x + ax^2 + b\dot{x}^2 + cx\dot{x} = 0\,. \tag{9}$$

How do we decide whether (9) is a good model for rhythmic finger movements? If a finger is moved back and forth, that is, performs an alternation between flexion and extension, then this process is to a good approximation symmetric: flexion is the mirror image of extension. In the equations a mirror operation is carried out by substituting x by $-x$, and, in doing so, the equation of motion must not change for symmetry to be preserved. Applied to (9) this leads to

$$\begin{aligned} &-\ddot{x} + \gamma(-\dot{x}) + \omega^2(-x) + a(-x)^2 + b(-\dot{x})^2 \\ &\quad + c(-x)(-\dot{x}) = 0 \\ &-\ddot{x} - \gamma\dot{x} - \omega^2 x + ax^2 + b\dot{x}^2 + cx\dot{x} = 0 \\ &\ddot{x} + \gamma\dot{x} + \omega^2 x - ax^2 - b\dot{x}^2 - cx\dot{x} = 0 \end{aligned} \tag{10}$$

where the last equation in (10) is obtained by multiplying the second equation by -1. It is evident that this equation is not the same as (9). In fact, it is only the same if $a = b = c = 0$, which means that there must not be any quadratic terms in the oscillator equation if one wants to preserve the symmetry between flexion and extension phases of movement. The argument goes even further: $N(x, \dot{x})$ must not contain any terms of even order in x and $\dot{x}$ as all of them, like the quadratic ones, would break the required symmetry. It is easy to convince oneself that as far as the flexion-extension symmetry is concerned all odd terms in x and $\dot{x}$ are fine.

There are four possible cubic terms, namely $\dot{x}^3$, $\dot{x}x^2$, $x\dot{x}^2$ and x^3 leading to a general oscillator equation of the form

$$\ddot{x} + \gamma\dot{x} + \omega^2 x + \delta\dot{x}^3 + \epsilon\dot{x}x^2 + ax^3 + bx\dot{x}^2 = 0\,. \tag{11}$$

The effects that these nonlinear terms exert on the oscillator dynamics can be best seen by rewriting (11) as

$$\ddot{x} + \dot{x}\underbrace{\{\gamma + \epsilon x^2 + \delta\dot{x}^2\}}_{\text{damping}} + x\underbrace{\{\omega^2 + ax^2 + b\dot{x}^2\}}_{\text{frequency}} = 0 \tag{12}$$

which shows that the terms $\dot{x}^3$ and $\dot{x}x^2$ are position and velocity dependent changes to the damping constant γ, whereas the nonlinearities x^3 and $x\dot{x}^2$ mainly influence the frequency. As the nonlinear terms were introduced to obtain stable limit cycles and the main interest is in amplitude and not frequency, we will let $a = b = 0$, which reduces the candidate oscillators to

$$\ddot{x} + \dot{x}\{\gamma + \epsilon x^2 + \delta\dot{x}^2\} + \omega^2 x = 0\,. \tag{13}$$

Nonlinear oscillators with either $\delta = 0$ or $\epsilon = 0$ have been studied for a long time and have been termed in the literature as van-der-Pol and Rayleigh oscillators, respectively.

Systems of the form (13) only show sustained oscillations on a stable limit cycle within certain ranges of the parameters, as can be seen easily for the van-der-Pol oscillator, given by (13) with $\delta = 0$

$$\ddot{x} + \dot{x}\underbrace{\{\gamma + \epsilon x^2\}}_{\tilde{\gamma}} + \omega^2 x = 0\,. \tag{14}$$

The underbraced term in (14) represents the effective damping constant, $\tilde{\gamma}$, now depending on the square of the displacement, x^2, a quantity which is non-negative. For the parameters γ and ϵ one can distinguish the following four cases:

$\gamma > 0, \epsilon > 0$ The effective damping $\tilde{\gamma}$ is always positive. The trajectories are evolving towards the origin, which is a stable fixed point.

$\gamma < 0, \epsilon < 0$ The effective damping $\tilde{\gamma}$ is always negative. The system is unstable and the trajectories are evolving towards infinity.

$\gamma > 0, \epsilon < 0$ For small values of the amplitude x^2 the effective damping $\tilde{\gamma}$ is positive leading to even smaller amplitudes. For large values of x^2 the effective damping $\tilde{\gamma}$ is negative leading to a further increase in amplitude. The system evolves either towards the fixed point or towards infinity depending on the initial conditions.

$\gamma < 0, \epsilon > 0$ For small values of the amplitude x^2 the effective damping $\tilde{\gamma}$ is negative leading to an increase in amplitude. For large values of x^2 the effective damping $\tilde{\gamma}$ is positive and decreases the amplitude. The system evolves towards a stable limit cycle.

The main features for the van-der-Pol oscillator are shown in Fig. 3 with the time series (left), the phase space portrait (middle) and the power spectrum (right). The time series is not a sine function but has a fast rising increasing flank and a more shallow slope on the decreasing side. Such time series are called relaxation oscillations. The trajectory in phase space is closer to a rectangle than to a circle and the power spectrum shows pronounced peaks at the fundamental frequency ω and its odd higher harmonics $(3\omega, 5\omega, \ldots)$.

In contrast to the van-der-Pol case the damping constant $\tilde{\gamma}$ for the Rayleigh oscillator, the case $\epsilon = 0$ in (13), depends on the square of the velocity $\dot{x}^2$. Arguments similar to those above lead to the conclusion that the Rayleigh oscillator shows sustained oscillations for parameters $\gamma < 0$ and $\delta > 0$.

As shown in Fig. 4 the time series and trajectories of the Rayleigh oscillator also exhibit relaxation behavior, but in this case with a slow rise and fast drop. As for the van-der-Pol, the phase space portrait is almost rectangular but the long and short axes are switched. Again the power spectrum has peaks at the fundamental frequency and contains odd higher harmonics.

Evidently, taken by themselves neither the van-der-Pol nor Rayleigh oscillators are good models for human limb movement for at least two reasons, even though they fulfill one requirement for a model: they have stable limit cycles. First, human limb movements are almost sinusoidal and their trajectories have a circular or elliptical shape. Second, it has also been found in experiments with human subjects performing rhythmic limb movements that when the movement rate is increased the amplitude of the movement decreases linearly with frequency [25]. It can be shown that for the van-der-Pol oscillator the amplitude is independent of frequency and for the Rayleigh it decreases proportional to ω^{-2}, both in disagreement with the experimental findings.

It turns out that a combination of the van-der-Pol and Rayleigh oscillator, termed the hybrid oscillator of the form (13) fulfills all the above requirements if the parameters are chosen as $\gamma < 0$ and $\epsilon \approx \delta > 0$.

As shown in Fig. 5 the time series for the hybrid oscillator is almost sinusoidal and the trajectory is elliptical. The power spectrum has a single peak at the fundamental frequency. Moreover, the relation between the amplitude and frequency is a linear decrease in amplitude when the rate is increased as shown schematically in Fig. 6. Taken together, the hybrid oscillator is a good approximation for the trajectories observed experimentally in human limb movements.

The Coupling

As pointed out already, in a second step one has to find a coupling function between two hybrid oscillators that leads to the correct dynamics for the relative phase (2). The most common realization of a coupling between two oscillators is a spring between two pendulums, leading to a force proportional to the difference in locations $f_{12} = k[x_1(t) - x_2(t)]$. It can easily be shown, that such a coupling does not lead to the required dynamics on the relative phase level. In fact, several coupling terms have been suggested that do the trick, but none of them is very intuitive. The arguably easiest form, which is one of the possible couplings presented in the original HKB model [19], is given by

$$f_{12} = (\dot{x}_1 - \dot{x}_2)\{\alpha + \beta(x_1 - x_2)^2\}\,. \tag{15}$$

Combined with two of the hybrid oscillators, the dynamical system that describes the transition from anti-phase to

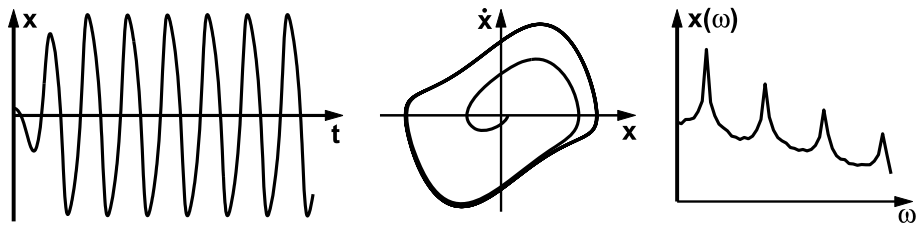

Movement Coordination, Figure 3
The van-der-Pol oscillator: time series (*left*), phase space trajectory (*middle*) and power spectrum (*right*)

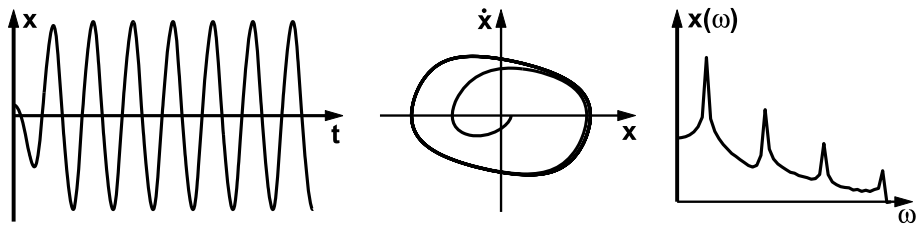

Movement Coordination, Figure 4
The Rayleigh oscillator: time series (*left*), phase space trajectory (*middle*) and power spectrum (*right*)

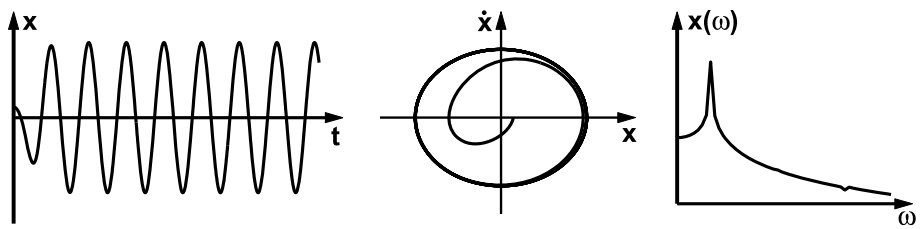

Movement Coordination, Figure 5
The hybrid oscillator: time series (*left*), phase space trajectory (*middle*) and power spectrum (*right*)

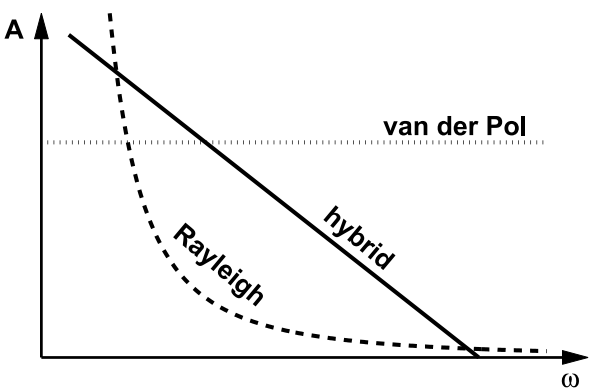

Movement Coordination, Figure 6
Amplitude-frequency relation for the van-der-Pol (*dotted*), Rayleigh ($\sim \omega^{-2}$, *dashed*) and hybrid ($\sim -\omega$, *solid*) oscillator

in-phase in bimanual finger movements takes the form

$$\begin{aligned} \ddot{x}_1 + \dot{x}_1\left(\gamma + \epsilon x_1^2 + \delta \dot{x}_1^2\right) + \omega^2 x_1 \\ = (\dot{x}_1 - \dot{x}_2)\left\{\alpha + \beta(x_1 - x_2)^2\right\} \\ \ddot{x}_2 + \dot{x}_2\left(\gamma + \epsilon x_2^2 + \delta \dot{x}_2^2\right) + \omega^2 x_2 \\ = (\dot{x}_2 - \dot{x}_1)\left\{\alpha + \beta(x_2 - x_1)^2\right\} . \end{aligned} \tag{16}$$

A numerical simulation of (16) is shown in Fig. 7. In the top row the amplitudes x_1 and x_2 are plotted as a function of time. The movement starts out in anti-phase at $\omega = 1.4$ and the frequency is continuously increased to a final value of $\omega = 1.8$. At a critical rate ω_c the anti-phase pattern becomes unstable and a transition to in-phase takes place. At the bottom a continuous estimate of the relative phase $\phi(t)$ is shown calculated as

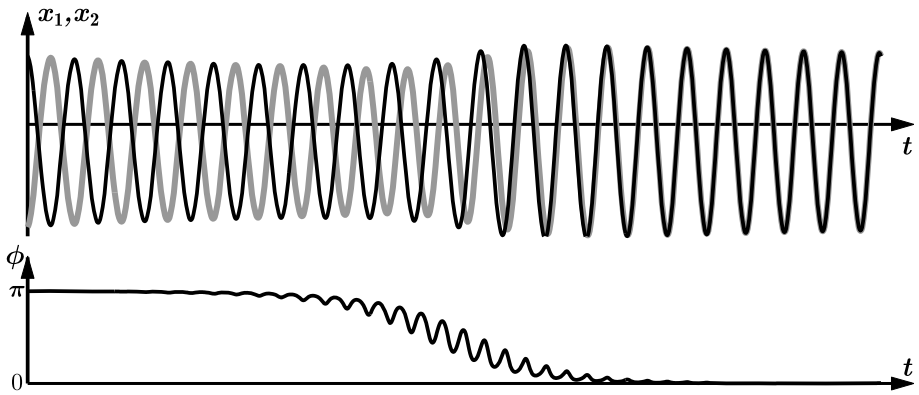

Movement Coordination, Figure 7
Simulation of (16) where the frequency ω is continuously increased from $\omega = 1.4$ on the left to $\omega = 1.8$ on the right. *Top*: time series of the amplitudes x_1 and x_2 undergoing a transition from anti-phase to in-phase when ω exceeds a critical value. *Bottom*: Continuous estimate of the relative phase ϕ changing from an initial value of π during anti-phase to 0 when the in-phase movement is established. Parameters: $\gamma = -0.7$, $\epsilon = \delta = 1$, $\alpha = -0.2$, $\beta = 0.2$, and $\omega = 1.4$ to 1.8

$$\phi(t) = \varphi_1(t) - \varphi_2(t) = \arctan\frac{\dot{x}_1}{x_1} - \arctan\frac{\dot{x}_2}{x_2}\,. \quad (17)$$

The relative phase changes from a value of π during the anti-phase movement to $\phi = 0$ when the in-phase pattern has been established.

To derive the phase relation (2) from (16) is a little lengthy but straightforward by using the ansatz (hypothesis)

$$x_k(t) = A_k(t)\mathrm{e}^{i\omega t} + A_k^*(t)\mathrm{e}^{-i\omega t} \quad (18)$$

then calculating the derivatives and inserting them into (16). Next a slowly varying amplitude approximation ($\dot{A}(t) \ll \omega$) and rotating wave approximation (neglect all frequencies $> \omega$) are applied. Finally, introducing the relative phase $\phi = \varphi_1 - \varphi_2$ after writing $A_k(t)$ in the form

$$A_k(t) = r\mathrm{e}^{i\varphi_k(t)} \quad (19)$$

leads to a relation for the relative phase ϕ of the form (2) from which the parameters a and b can be readily found in terms of the parameters that describe the oscillators and their coupling in (16)

$$a = -\alpha - 2\beta r^2\,, \quad b = \frac{1}{2}\beta r^2$$
$$\text{with} \quad r^2 = \frac{-\gamma + \alpha(1-\cos\phi)}{\epsilon + 3\delta\omega^2 - 2\beta(1-\cos\phi)^2}\,. \quad (20)$$

Breaking and Restoring Symmetries

Symmetry Breaking Through the Components

For simplicity, the original HKB model assumes on both the oscillator and the relative phase level that the two coordinating components are identical, like two index fingers. As a consequence, the coupled system (16) has a symmetry: it stays invariant if we replace x_1 by x_2 and x_2 by x_1. For the coordination between two limbs that are not the same like an arm and a leg, this symmetry no longer exists – it is said to be broken. In terms of the model, the main difference between an arm and a leg is that they have different eigenfrequencies, so the oscillator frequencies ω in (16) are no longer the same but become ω_1 and ω_2. This does not necessarily mean that during the coordination the components oscillate at different frequencies; they are still coupled, and this coupling leads to a common frequency Ω, at least as long as the eigenfrequency difference is not too big. But still, a whole variety of new phenomena originates from such a breaking of the symmetry between the components [5,22,23,29,37].

As mentioned in Subsect. "The Coupling" the dynamics for the relative phase can be derived from the level of coupled oscillators (16) for the case of the same eigenfrequencies. Performing the same calculations for two oscillators with frequencies ω_1 and ω_2 leads to an additional term in (2), which turns out to be a constant, commonly called $\delta\omega$. With this extension the equation for the relative phase reads

$$\dot{\phi} = \delta\omega - a\sin\phi - 2b\sin 2\phi$$
$$\text{with} \quad \delta\omega = \frac{\omega_1^2 - \omega_2^2}{\Omega} \approx \omega_1 - \omega_2\,. \quad (21)$$

The exact form for the term $\delta\omega$ turns out to be the difference of the squares of the eigenfrequencies divided by the rate Ω the oscillating frequency of the coupled system, which simplifies to $\omega_1 - \omega_2$ if the frequency difference is small. As before (21) can be scaled, which eliminates one

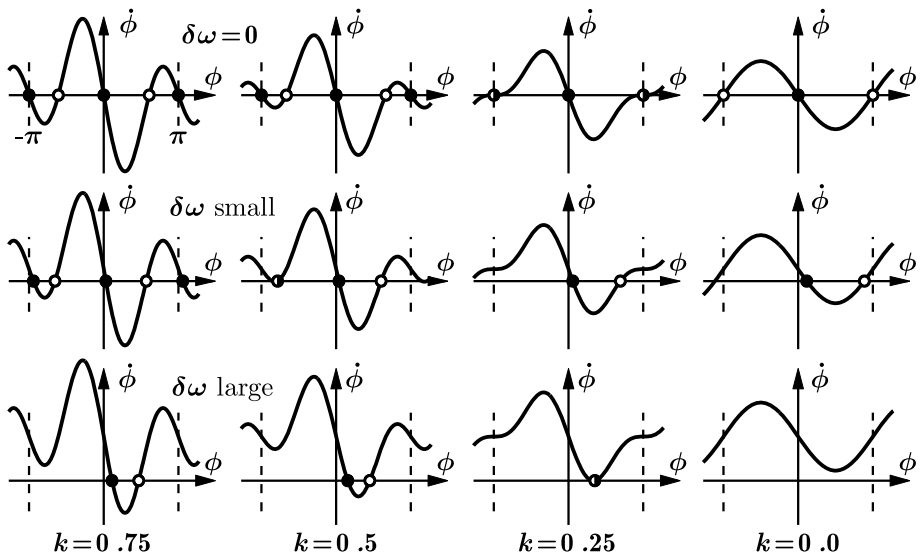

Movement Coordination, Figure 8
Phase space plots for different values of the control parameters k and $\delta\omega$. With increasing asymmetry (*top* to *bottom*) the functions are shifted more and more upwards leading to an elimination of the fixed points near $\phi = -\pi$ and $\phi = 0$ via saddle node bifurcations at $k = 0.5$ for small $\delta\omega$ and $k = 0.25$ for $\delta\omega$ large, respectively

of the parameters, and $\dot{\phi}$ can be derived from a potential function

$$\dot{\phi} = \delta\omega - \sin\phi - 2k\sin 2\phi = -\frac{\mathrm{d}V(\phi)}{\mathrm{d}\phi} \text{ with } V(\phi) = -\delta\omega\,\phi - \cos\phi - k\cos 2\phi\,. \tag{22}$$

Plots of the phase space and the potential landscape for different values of k and $\delta\omega$ are shown in Figs. 8 and 9, respectively. From these figures it is obvious that the symmetry breaking leads to a vertical shift of the curves in phase space and a tilt in the potential functions, which has several important consequences for the dynamics. First, for a nonvanishing $\delta\omega$ the stable fixed points for the relative phase are no longer located at $\phi = 0$ and $\phi = \pm\pi$ but are now shifted (see Fig. 8). The amount of this shift can be calculated for small values of $\delta\omega$ and new locations for the stable fixed points are given by

$$\phi^{(0)} = \frac{\delta\omega}{1+4k} \quad \text{and} \quad \phi^{(\pi)} = \pi - \frac{\delta\omega}{1-4k}\,. \tag{23}$$

Second, for large enough values of $\delta\omega$ not only the fixed point close to $\phi = \pi$ becomes unstable but also the in-phase pattern loses stability undergoing a saddle node bifurcation as can be seen in the bottom row in Fig. 8. Beyond this point there are no stable fixed points left and the relative phase will not settle down at a fixed value anymore but exhibits phase wrapping. However, this wrapping does not occur with a constant angular velocity, which can best be seen in the plot on the bottom right in Fig. 9. As the change in relative phase $\dot{\phi}$ is the negative derivative of the potential function, it is given by the slope. This slope is large and almost constant for negative values of ϕ, but for small positive values, where the in-phase fixed point was formerly located, the slope becomes less steep indicating that ϕ changes more slowly in this region before the dynamics picks up speed again when approaching π. So even as the fixed point has disappeared the dynamics still shows reminiscence of its former existence.

The dynamics of relative phase for the case of different eigenfrequencies from a simulation of (22) in shown in Fig. 10. Starting out at a slow movement rate on the left, the system settles into the fixed point close to $\phi = \pi$. When the movement rate is continuously increased, the fixed point drifts upwards. At a first critical point a transition to in-phase takes place, followed by another drift, this time for the fixed point representing the in-phase movement. Finally, this state also looses stability and the relative phase goes into wrapping. Reminiscence in the phase regions of the former fixed point are still visible by a flattening of the slope around $\phi \approx> 0$. With a further increase of the movement rate the function approaches a straight line.

The third consequence of this symmetry breaking is best described using the potential function for small values of $\delta\omega$ compared to the symmetric case $\delta\omega = 0$. For the lat-

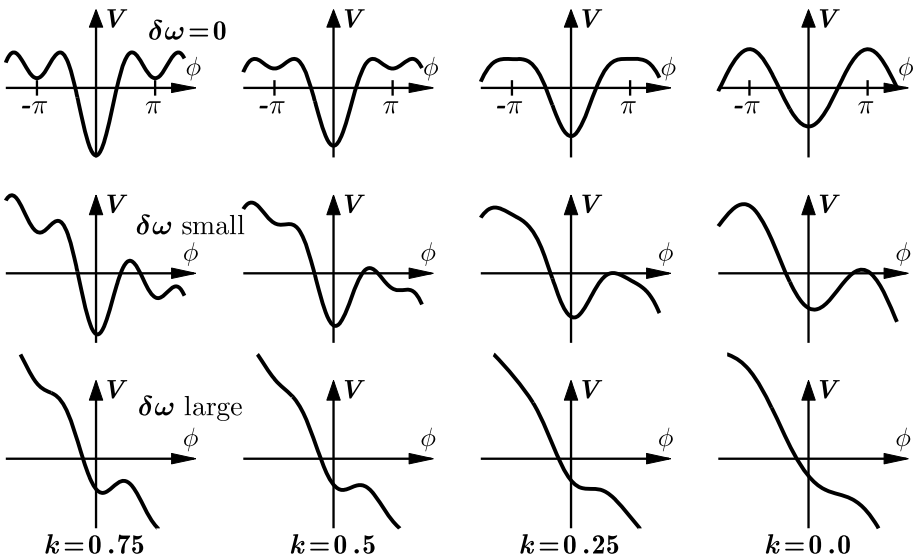

Movement Coordination, Figure 9

Potential landscape for different values of the control parameters k and $\delta\omega$. With increasing asymmetry (*top* to *bottom*) the functions get more and more tilted, destabilizing the system up to a point where there are no fixed points left on the bottom right. However, remnants of the fixed point can still be seen as changes in the curvature of the potential

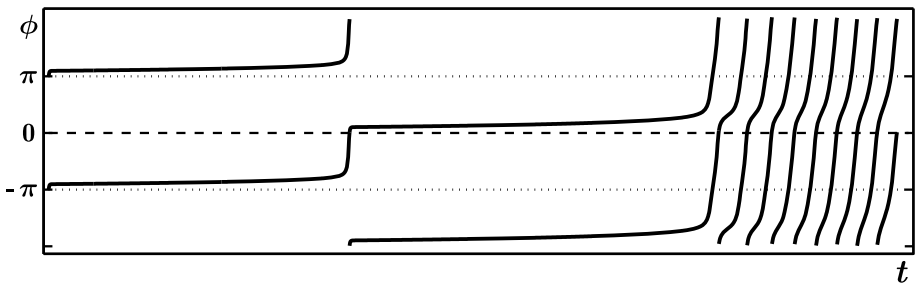

Movement Coordination, Figure 10

Relative phase ϕ as a function of time. Shown is a 4-π plot of a simulation of (22) for $\delta\omega = 1.7$ where the control parameter k is continuously decreased from $k = 2$ on the left to $k = 0$ on the right. The system settles close to anti-phase and the fixed point drifts as k is decreased (corresponding to a faster period of oscillation). At a first critical value a transition to in-phase takes place followed by another fixed point drift. Finally, the in-phase fixed point disappears and the phase starts wrapping

ter, when the system is initially in anti-phase $\phi = \pi$ and k is decreased through its critical value a switch to in-phase takes place as was shown in Fig. 1 (middle row). However, the ball there does not necessarily have to roll to the left towards $\phi = 0$ but with the same probability could roll to the right ending up in the minimum that exists at $\phi = 2\pi$ and also represents an in-phase movement. Whereas the eventual outcome is the same because due to the periodicity $\phi = 0$ and $\phi = 2\pi$ are identical, the two paths can very well be distinguished. The curve in Fig. 7 (bottom), showing the continuous estimate of the relative phase during a transition, goes from $\phi = \pi$ down to $\phi = 0$, but could, in fact with the same probability, go up towards $\phi = 2\pi$.

In contrast, if the eigenfrequencies are different, also the points $-\pi$ and π, and 0 and 2π are no longer the same. If the system is in anti-phase at $\phi = \pi$ and k is decreased, it is evident from the middle row in Fig. 9 that a switch will not take place towards the left to $\phi \approx 0$, as the dynamics would have to climb over a potential hill to do so. As there are random forces acting on the dynamics a switch to $\phi \approx 0$ will still happen from time to time, but it is not equally probable to a transition to $\phi \approx 2\pi$, and it becomes even more unlikely with increasing $\delta\omega$.

These consequences, theoretically predicted to occur when the symmetry between the oscillating components is broken, can and have been tested, and have been found to

be in agreement with the experimental results [21,29] (see also [32,41]).

Asymmetry in the Mode of Coordination

Even though (16) is symmetric in the coordinating components it can only describe a transition from anti-phase to in-phase but not the other way around. Equation (16) is highly asymmetric with respect to coordination mode. This can be seen explicitly when we introduce variables that directly reflect modes of coordination

$$\psi_+ = x_1 + x_2 \quad \text{and} \quad \psi_- = x_1 - x_2 \,. \tag{24}$$

For an in-phase movement we have $x_1 = x_2$ and ψ_- vanishes, whereas for anti-phase $x_1 = -x_2$ and therefore $\psi_+ = 0$. We can now derive the dynamics in the variables ψ_+ and ψ_- by expressing the original displacements as

$$x_1 = \frac{1}{2}(\psi_+ + \psi_-) \quad \text{and} \quad x_2 = \frac{1}{2}(\psi_+ - \psi_-) \tag{25}$$

and inserting them into (16), which leads to

$$\begin{aligned} &\ddot{\psi}_+ + \epsilon\dot{\psi}_+ + \omega^2\psi_+ + \frac{\gamma}{12}\frac{\mathrm{d}}{\mathrm{d}t}\left(\psi_+^3 + 3\psi_+\psi_-^2\right) \\ &\quad + \frac{\delta}{4}\left(\dot{\psi}_+^3 + 3\dot{\psi}_+\dot{\psi}_-^2\right) = 0 \\ &\ddot{\psi}_- + \epsilon\dot{\psi}_- + \omega^2\psi_- + \frac{\gamma}{12}\frac{\mathrm{d}}{\mathrm{d}t}\left(\psi_-^3 + 3\psi_-\psi_+^2\right) \\ &\quad + \frac{\delta}{4}\left(\dot{\psi}_-^3 + 3\dot{\psi}_-\dot{\psi}_+^2\right) = 2\dot{\psi}_-\left(\alpha + \beta\psi_-^2\right) . \end{aligned} \tag{26}$$

The asymmetry between in-phase and anti-phase is evident from (26), as the right-hand side of the first equation vanishes and the equation is even independent of the coupling parameters α and β. This is the reason that the original HKB model only shows transitions from anti-phase to in-phase and not vice versa.

Transitions to Anti-phase

In 2000 Carson and colleagues [6] published results from an experiment in which subjects performed bimanual pronation-supination movements paced by a metronome of increasing rate (see also [2]). In this context an anti-phase movement corresponds to the case where one arm performs a pronation while the other arm is supinating. Correspondingly, pronation and supination with both arms at the same time represents in-phase. In their experiment Carson et al. used a manipulandum that allowed for changing the axis of rotation individually for both arms as shown in Fig. 11a. With increasing movement rate spontaneous transitions from anti-phase to in-phase, but not vice versa, were found when the subjects performed pronation-supination movements around the same axes for both arms. In trials where one arm was rotating around the axis above the hand and the other around the one below, anti-phase was found to be stable and the in-phase movement underwent a transition to anti-phase as shown for representative trials in Fig. 12.

It is evident that the HKB model in neither its original form (2) nor the mode formulation (26) is a valid model for these findings. However, Fuchs and Jirsa [11] showed that by starting from the mode description (26) it is straightforward to extend HKB such that, depending on an additional parameter σ, either the in-phase or the anti-

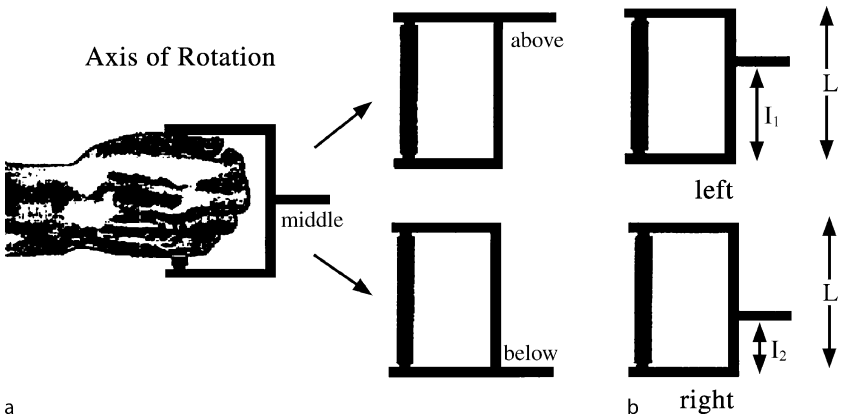

Movement Coordination, Figure 11

Manipulandum used by Carson and colleagues [6]. a The original apparatus that allowed for variation in axis of rotation above, below and in the middle of the hand. b The axis of rotation can be changed continuously, allowing us to introduce a parameter σ as a quantitative measure for the relative locations of the axes

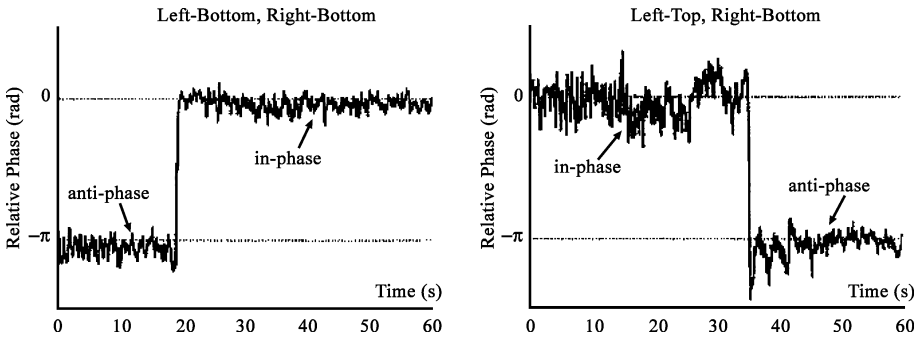

Movement Coordination, Figure 12
Relative phase over time for two representative trials from the Carson et al. experiment. *Left*: the axis of rotation is below the hand for both arms and a switch from anti-phase to in-phase occurs as the movement speeds up. *Right*: with one axis above and the other below the hand, the in-phase movement becomes unstable at higher rates leading to a transition to anti-phase

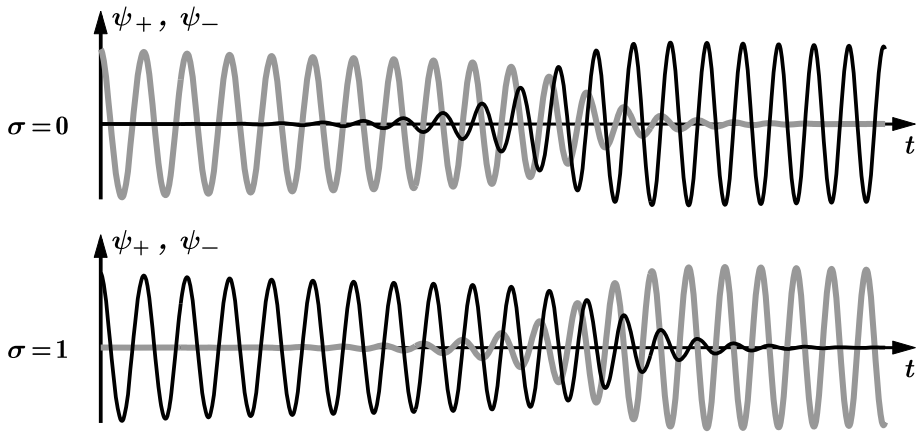

Movement Coordination, Figure 13
Simulation of (28) for $\sigma = 0$ (*top*) and $\sigma = 1$ (*bottom*) where the frequency ω is continuously increased from $\omega = 1.4$ on the left to $\omega = 1.8$ on the right. Time series of the mode amplitudes ψ_+ (black) and ψ_- (gray) undergoing transitions from anti-phase to in-phase (*top*) and from in-phase to anti-phase (*bottom*) when ω exceeds a critical value. Parameters: $\gamma = -0.7, \epsilon = \delta = 1, \alpha = -0.2$, $\beta = 0.2$, and $\omega = 1.4$ to 1.8

phase mode is a stable movement pattern at high rates. The additional parameter corresponds to the relative locations of the axes of rotation in the Carson et al. experiment which can be defined in its easiest form as

$$\sigma = \frac{|l_1 - l_2|}{L} \tag{27}$$

where l_1, l_2 and L are as shown in Fig. 11b. In fact, any monotonic function f with $f(0) = 0$ and $f(1) = 1$ is compatible with theory and its actual shape has to be determined experimentally.

By looking at the mode Eqs. (26) it is clear that a substitution $\psi_+ \to \psi_-$ and $\psi_- \to \psi_+$ to the left-hand side of the first equation leads to the left-hand side of the second equation and vice versa. For the terms on the right-hand side representing the coupling this is obviously not the case. Therefore, we now introduce a parameter σ and additional terms into (26) such that for $\sigma = 0$ these equations remain unchanged, whereas for $\sigma = 1$ we obtain (26) with all + and − subscripts reversed

$$\begin{aligned}
&\ddot{\psi}_+ + \epsilon\dot{\psi}_+ + \omega^2\psi_+ + \frac{\gamma}{12}\frac{\mathrm{d}}{\mathrm{d}t}\left(\psi_+^3 + 3\psi_+\psi_-^2\right) \\
&\qquad + \frac{\delta}{4}\left(\dot{\psi}_+^3 + 3\dot{\psi}_+\dot{\psi}_-^2\right) = 2\sigma\dot{\psi}_+\left(\alpha + \beta\psi_+^2\right) \\
&\ddot{\psi}_- + \epsilon\dot{\psi}_- + \omega^2\psi_- + \frac{\gamma}{12}\frac{\mathrm{d}}{\mathrm{d}t}\left(\psi_-^3 + 3\psi_-\psi_+^2\right) \\
&\qquad + \frac{\delta}{4}\left(\dot{\psi}_-^3 + 3\dot{\psi}_-\dot{\psi}_+^2\right) = 2(1-\sigma)\dot{\psi}_-\left(\alpha + \beta\psi_-^2\right).
\end{aligned} \tag{28}$$

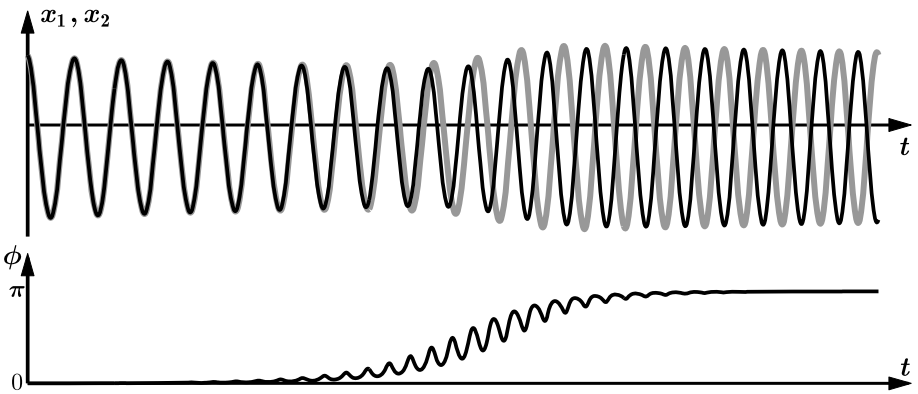

Movement Coordination, Figure 14
Simulation of (30) where the frequency ω is continuously increased from $\omega = 1.4$ on the left to $\omega = 1.8$ on the right. *Top*: time series of the amplitudes x_1 and x_2 undergoing a transition from in-phase to anti-phase when ω exceeds a critical value. *Bottom*: Continuous estimate of the relative phase ϕ changing from an initial value of 0 during the in-phase to π when the anti-phase movement is established. Parameters: $\gamma = -0.7, \epsilon = \delta = 1, \alpha = -0.2, \beta = 0.2, \sigma = 1$ and $\omega = 1.4$ to 1.8

From (28) it is straight forward to go back to the representation of the limb oscillators

$$\begin{aligned}\ddot{x}_1 + \ldots &= \frac{1}{2}\left(\ddot{\psi}_+ + \ddot{\psi}_-\right) + \ldots \\ &= \dot{\psi}_-\left(\alpha + \beta\psi_-^2\right) + \sigma\left\{\dot{\psi}_+\left(\alpha + \beta\psi_+^2\right)\right. \\ &\qquad \left. - \dot{\psi}_-\left(\alpha + \beta\psi_-^2\right)\right\} \\ \ddot{x}_2 + \ldots &= \frac{1}{2}\left(\ddot{\psi}_+ - \ddot{\psi}_-\right) + \ldots \\ &= -\dot{\psi}_-\left(\alpha + \beta\psi_-^2\right) + \sigma\left\{\dot{\psi}_+\left(\alpha + \beta\psi_+^2\right)\right. \\ &\qquad \left. + \dot{\psi}_-\left(\alpha + \beta\psi_-^2\right)\right\}\end{aligned} \tag{29}$$

where the left-hand side which represents the oscillators has been written only symbolically as all we are dealing with is the coupling on the right. Replacing the mode amplitudes ψ_+ and ψ_- in (29) using (24) one finds the generalized coupling as a function of x_1 and x_2

$$\begin{aligned}\ddot{x}_1 + \ldots &= (\dot{x}_1 - \dot{x}_2)\left\{\alpha + \beta(x_1 - x_2)^2\right\} \\ &\quad + 2\sigma\left\{\alpha\dot{x}_2 + \beta\left[\dot{x}_2\left(x_1^2 + x_2^2\right) + 2\dot{x}_1 x_1 x_2\right]\right\} \\ \ddot{x}_2 + \ldots &= (\dot{x}_2 - \dot{x}_1)\left\{\alpha + \beta(x_2 - x_1)^2\right\} \\ &\quad + 2\sigma\left\{\alpha\dot{x}_1 + \beta\left[\dot{x}_1\left(x_1^2 + x_2^2\right) + 2\dot{x}_2 x_1 x_2\right]\right\} .\end{aligned} \tag{30}$$

Like the original oscillator Eq. (16), Eq. (30) is invariant under the exchange of x_1 and x_2 but in addition allows for transitions from in-phase to anti-phase coordination if the parameter σ is chosen appropriately ($\sigma = 1$, for instance), as shown in Fig. 14.

As the final step, an equation for the dynamics of relative phase can be obtained from (30) by performing the same steps as before, which leads to a modified form of the HKB equation (2)

$$\dot{\phi} = -(1 - 2\sigma)a\sin\phi - 2b\sin 2\phi \tag{31}$$

and the corresponding potential function

$$\begin{aligned}\dot{\phi} &= -\frac{\mathrm{d}V(\phi)}{\mathrm{d}\phi} \\ \text{with} \quad V(\phi) &= -(1 - 2\sigma)a\cos\phi - b\cos 2\phi .\end{aligned} \tag{32}$$

Both equations can be scaled again leading to

$$\begin{aligned}\dot{\phi} &= -(1 - 2\sigma)\sin\phi - 2k\sin 2\phi \\ &= -\frac{\mathrm{d}V(\phi)}{\mathrm{d}\phi} \quad \text{with} \\ V(\phi) &= -(1 - 2\sigma)\cos\phi - k\cos 2\phi .\end{aligned} \tag{33}$$

The landscapes of the potential for different values of the control parameters k and σ are shown in Fig. 15. The left column exhibits the original HKB case which is obtained for $\sigma = 0$. The functions in the most right column, representing the situation for $\sigma = 1$, are identical in shape to the $\sigma = 0$ case, simply shifted horizontally by a value of π. These two extreme cases are almost trivial and were the ones originally investigated in the Carson et al. experiment with the axes of rotation either on the same side or on opposite sides with respect to the hand. As the corresponding potential functions are shifted by π with respect to each other, one could assume that for an intermediate value of σ between 0 and 1 the functions are also shifted, just by a smaller amount. Such horizontal translations lead to fixed point drifts, as has been seen before for oscillation components with different eigenfrequen-

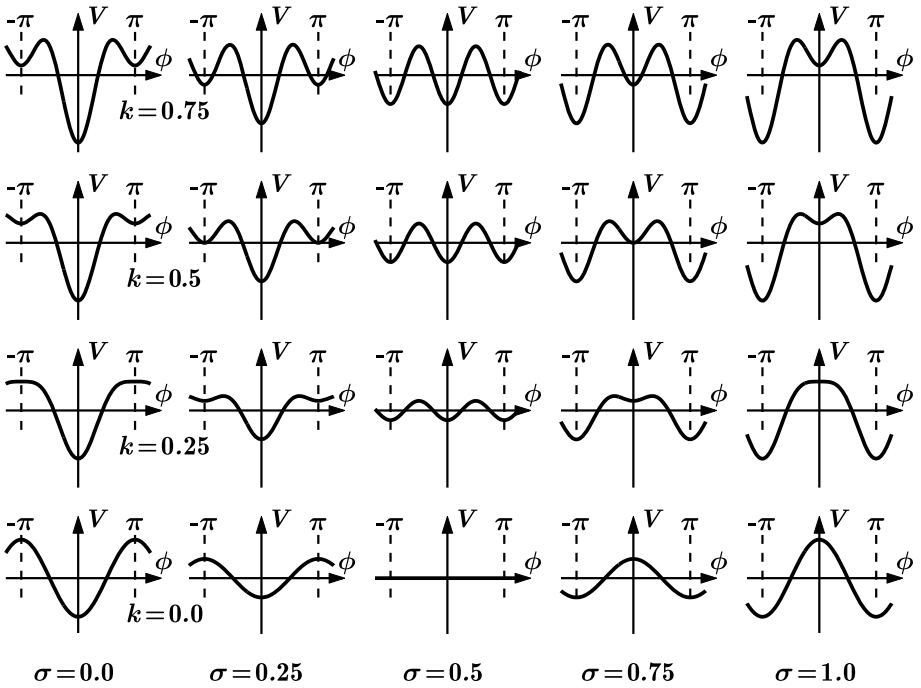

Movement Coordination, Figure 15
Potential landscape for different values of the control parameters *k* and *σ*

cies. The theory, however, predicts that this is not the case. In fact, for $\sigma = 0.5$ theory predicts that the two coordination modes in-phase and anti-phase are equally stable for all movement rates. The deep minima for slow rates indicate high stability for both movement patterns and as the rate increases both minima become more and more shallow, i. e. both movement patterns become less stable. Eventually, for high rates at $k = 0$ the potential is entirely flat, which means that there are no attractive states whatsoever. Pushed only by the stochastic forces in the system, the relative phase will now undergo a random walk. Note that this is very different from the phase wrapping encountered before where the phase was constantly increasing due to the lack of an attractive state. Here the relative phase will move back and forth in a purely random fashion, known in the theory of stochastic systems as Brownian motion. Again experimental evidence exists from the Carson group that changing the distance between the axes of rotation gradually leads to the phenomena predicted by theory.

Conclusions

The theoretical framework outlined above represents the core of the dynamical systems approach to movement coordination. Rather than going through the large variety of phenomena that coordination dynamics and the HKB model have been applied to, emphasis has been put on a detailed description of the close connection between theoretical models and experimental results. Modeling the coordination of movement as dynamical systems on both the mesoscopic level of the component oscillators and the macroscopic level of relative phase allowed for quantitative predictions and experimental tests with an accuracy that is virtually unprecedented in the life sciences, a field where most models are qualitative and descriptive.

Extensions of the HKB Model

Beyond the phenomena described above, the HKB model has been extended in various ways. Some of these extensions (by no mean exhaustive) are listed below with very brief descriptions; the interested reader is referred to the literature for details.

- The quantitative description of the influence of noise on the dynamics given in Sect. "Stability: Perturbations and Fluctuations" can be done in a quantitative fashion by adding a stochastic term to (2) [40,43] or its generalizations (21) and (31) [11] and treating them as Langevin equations within the theory of stochastic systems (see e. g. [16] for stochastic systems). In this case the system is no longer described by a single time series for the relative phase but by a probability distribu-

tion function. How such distributions evolve in time is then given by the corresponding Fokker–Planck equation and allows for a quantitative description of the stochastic phenomena such as enhancement of fluctuations and critical fluctuations. An important quantity that can be derived in this context and is also related to the critical fluctuations is the mean-first-passage time, which is the time it takes (on average) to move over a hump in the potential function.

- When subjects flex a single finger between the beats of a metronome, i. e. syncopate with the stimulus, and the metronome rate is increased, they switch spontaneously to a coordination pattern where they flex their finger on the beat, i. e. synchronize with the stimulus. This so-called syncopation-synchronization paradigm introduced by Kelso and colleagues [32] has been frequently used in brain-imaging experiments.
- A periodic patterning in the time series of the relative phase was found experimentally in the case of broken symmetry by Schmidt et al. [41] and successfully derived from the oscillator level of the HKB model [12,14].
- The metronome pacing can be explicitly included into (2) and its generalizations [24]. This so-called parametric driving allows us to explain effects in the movement trajectory known as anchoring, i. e. the variability of the movement is smaller around the metronome beat compared to other regions in phase space [10]. With parametric driving the HKB model also makes correct predictions for the stability of multi-frequency coordination, where the metronome cycle is half of the movement cycle, i. e. there is a beat at the points of maximum flexion and maximum extension [1]. There are also effects from more complicated polyrhythms that have been studied [38,39,47,48,49].
- The effect of symmetry breaking has been studied intensively in experiments where subjects were swinging pendulums with different eigenfrequencies [8,37,46].
- Transitions are also found in trajectory formation, for instance when subjects move their index finger such that they draw an "8" and this movement is sped up the pattern switches to a "0" [3,4,9].

Future Directions

One of the most exciting applications of movement coordination and its spontaneous transitions in particular is that they open a new window for probing the human brain, made possible by the rapid development of brain-imaging technologies that allow for the recording of brain activity in a noninvasive way. Electroencephalography (EEG), magnetoencephalography (MEG) and functional magnetic resonance tomography (fMRI) have been used in coordination experiments since the 1990s to study the changes in brain activations accompanying (or triggering?) the switches in movement behavior [13,33,34]. Results from MEG experiments reveal a strong frequency dependence of the dominating pattern with the contribution of the auditory system being strongest at low metronome/movement rates, whereas at high rates the signals from sensorimotor cortex dominate [15,35]. The crossover point is found at rates around 2 Hz, right where the transitions typically take place.

In two other studies the rate dependence of the auditory and sensorimotor system was investigated separately. In an MEG experiment Carver et al. [7] found a resonance-like enhancement of a brain response that occurs about 50 ms after a tone is delivered, again at a rate of about 2 Hz. In the sensorimotor system a nonlinear effect of rate was shown as well. Using a continuation paradigm, where subjects moved an index finger paced by a metronome which was turned off at a certain time while the subjects were to continue moving at the same rate, Mayville et al. [36] showed that a certain pattern of brain activation drops out when the movement rate exceeds about 1.5 Hz. Even though their contribution to behavioral transitions is far from being completely understood, it is clear that such nonlinear effects of rate exist in both the auditory and the sensorimotor system in parameter regions where behavioral transitions are observed.

Using fMRI brain areas have been identified that show a dependence of their activation level as a function of rate only, independent of coordination mode, whereas activation in other areas strongly depends on whether subjects are syncopating or synchronizing regardless of how fast they are moving [20].

Taken together, these applications of coordination dynamics to brain research have hardly scratched the surface so far but the results are already very exciting as they demonstrate that the experimental paradigms from movement coordination may be used to prepare the brain into a certain state where its responses can be studied. With further improvement of the imaging technologies and analysis procedures many more results can be expected to contribute significantly to our understanding of how the human brain works.

Acknowledgment

Work reported herein was supported by NINDS grant 48299, NIMH grants 42900 and 80838, and the Pierre de Fermat Chair to J.A.S.K.

Bibliography

Primary Literature

1. Assisi CG, Jirsa VK, Kelso JAS (2005) Dynamics of multifrequency coordination using parametric driving: Theory and Experiment. Biol Cybern 93:6–21
2. Buchanan JJ, Kelso JAS (1993) Posturally induced transitions in rhythmic multijoint limb movements. Exp Brain Res 94:131–142
3. Buchanan JJ, Kelso JAS, Fuchs A (1996) Coordination dynamics of trajectory formation. Biol Cybern 74:41–54
4. Buchanan JJ, Kelso JAS, DeGuzman GC (1997) The self-organization of trajectory formation: I. Experimental evidence. Biol Cybern 76:257–273
5. Carson RG, Goodman D, Kelso JAS, Elliott D (1995) Phase transitions and critical fluctuations in rhythmic coordination of ipsilateral hand and foot. J Mot Behav 27:211–224
6. Carson RG, Rick S, Smethrust CJ, Lison JF, Biblow WD (2000) Neuromuscular-skeletal constraints upon the dynamics of unimanual and bimanual coordination. Exp Brain Res 131:196–214
7. Carver FW, Fuchs A, Jantzen KJ, Kelso JAS (2002) Spatiotemporal analysis of neuromagnetic activity associated with rhythmic auditory stimulation. Clin Neurophysiol 113:1909–1920
8. Collins DR, Sternad D, Turvey MT (1996) An experimental note on defining frequency competition in intersegmental coordination dynamics. J Mot Behav 28:299–303
9. DeGuzman GC, Kelso JAS, Buchanan JJ (1997) The self-organization of trajectory formation: II. Theoretical model. Biol Cybern 76:275–284
10. Fink P, Kelso JAS, Jirsa VK, Foo P (2000) Local and global stabilization of coordination by sensory information. Exp Brain Res 134:9–20
11. Fuchs A, Jirsa VK (2000) The HKB model revisited: How varying the degree of symmetry controls dynamics. Hum Mov Sci 19:425–449
12. Fuchs A, Kelso JAS (1994) A theoretical note on models of Interlimb coordination. J Exp Spychol Hum Percept Perform 20:1088–1097
13. Fuchs A, Kelso JAS, Haken H (1992) Phase transitions in the human brain: Spatial mode dynamics. Int J Bifurc Chaos 2:917–939
14. Fuchs A, Jirsa VK, Haken H, Kelso JAS (1996) Extending the HKB-Model of coordinated movement to oscillators with different eigenfrequencies. Biol Cybern 74:21–30
15. Fuchs A, Mayville JM, Cheyne D, Weinberg H, Deecke L, Kelso JAS (2000) Spatiotemporal Analysis of Neuromagnetic Events Underlying the Emergence of Coordinative Instabilities. NeuroImage 12:71–84
16. Gardiner CW (1985) Handbook of stochastic Systems. Springer, Heidelberg
17. Haken H (1977) Synergetics, an introduction. Springer, Heidelberg
18. Haken H (1983) Advanced Synergetics. Springer, Heidelberg
19. Haken H, Kelso JAS, Bunz H (1985) A theoretical model of phase transition in human hand movements. Biol Cybern 51:347–356
20. Jantzen KJ, Kelso JAS (2007) Neural coordination dynamics of human sensorimotor behavior: A review. In: Jirsa VK, McIntosh AR (eds) Handbook of Brain Connectivity. Springer, Heidelberg
21. Jeka JJ, Kelso JAS (1995) Manipulating symmetry in human two-limb coordination dynamics. J Exp Psychol Hum Percept Perform 21:360–374
22. Jeka JJ, Kelso JAS, Kiemel T (1993) Pattern switching in human multilimb coordination dynamics. Bull Math Biol 55:829–845
23. Jeka JJ, Kelso JAS, Kiemel T (1993) Spontaneous transitions and symmetry: Pattern dynamics in human four limb coordination. Hum Mov Sci 12:627–651
24. Jirsa VK, Fink P, Foo P, Kelso JAS (2000) Parameteric stabilization of biological coordination: a theoretical model. J Biol Phys 26:85–112
25. Kay BA, Kelso JAS, Saltzman EL, Schöner G (1987) Space-time behavior of single and bimanual rhythmic movements: Data and limit cycle model. J Exp Psychol Hum Percept Perform 13:178–192
26. Kay BA, Saltzman EL, Kelso JAS (1991) Steady state and perturbed rhythmical movements: Dynamical modeling using a variety of analytic tools. J Exp Psychol Hum Percept Perform 17:183–197
27. Kelso JAS (1981) On the oscillatory basis of movement. Bull Psychon Soc 18:63
28. Kelso JAS (1984) Phase transitions and critical behavior in human bimanual coordination. Am J Physiol Regul Integr Comp 15:R1000–R1004
29. Kelso JAS, Jeka JJ (1992) Symmetry breaking dynamics of human multilimb coordination. J Exp Psychol Hum Percept Perform 18:645–668
30. Kelso JAS, Scholz JP, Schöner G (1986) Nonequilibrium phase transitions in coordinated biological motion: Critical fluctuations. Phys Lett A 118:279–284
31. Kelso JAS, Schöner G, Scholz JP, Haken H (1987) Phase locked modes, phase transitions and component oscillators in coordinated biological motion. Phys Scr 35:79–87
32. Kelso JAS, DelColle J, Schöner G (1990) Action-perception as a pattern forming process. In: Jannerod M (ed) Attention and performance XIII. Erlbaum, Hillsdale, pp 139–169
33. Kelso JAS, Bressler SL, Buchanan S, DeGuzman GC, Ding M, Fuchs A, Holroyd T (1992) A phase transition in human brain and behavior. Phys Lett A 169:134–144
34. Kelso JAS, Fuchs A, Holroyd T, Lancaster R, Cheyne D, Weinberg H (1998) Dynamic cortical activity in the human brain reveals motor equivalence. Nature 392:814–818
35. Mayville JM, Fuchs A, Ding M, Cheyne D, Deecke L, Kelso JAS (2001) Event-related changes in neuromagnetic activity associated with syncopation and synchronization timing tasks. Hum Brain Mapp 14:65–80
36. Mayville JM, Fuchs A, Kelso JAS (2005) Neuromagnetic motor fields accompanying self-paced rhythmic finger movements of different rates. Exp Brain Res 166:190–199
37. Park H, Turvey MT (2008) Imperfect symmetry and the elementary coordination law. In: Fuchs A, Jirsa VK (eds) Coordination: Neural, Behavioral and Social Dynamics. Springer, Heidelberg, pp 3–25
38. Peper CE, Beek PJ (1998) Distinguishing between the effects of frequency and amplitude on interlimb coupling in tapping a 2:3 polyrhythm. Exp Brain Res 118:78–92
39. Peper CE, Beek PJ, van Wieringen PC (1995) Frequency-induced phase transitions in bimanual tapping. Biol Cybern 73:303–309
40. Post AA, Peeper CE, Daffertshofer A, Beek PJ (2000) Relative phase dynamics in perturbed interlimb coordination: stability and stochasticity. Biol Cybern 83:443–459

41. Schmidt RC, Beek PJ, Treffner PJ, Turvey MT (1991) Dynamical substructure of coordinated rhythmic movements. J Exp Psychol Hum Percept Perform 17:635–651
42. Schöner G, Kelso JAS (1988) Dynamic pattern generation in behavioral and neural systems. Science 239:1513–1520
43. Schöner G, Haken H, Kelso JAS (1986) A stochastic theory of phase transitions in human hand movements. Biol Cybern 53:442–453
44. Scholz JP, Kelso JAS (1989) A quantitative approach to understanding the formation and change of coordinated movement patterns. J Mot Behav 21:122–144
45. Scholz JP, Kelso JAS, Schöner G (1987) Nonequilibrium phase transitions in coordinated biological motion: Critical slowing down and switching time. Phys Lett A 8:90–394
46. Sternad D, Collins D, Turvey MT (1995) The detuning factor in the dynamics of interlimb rhythmic coordination. Biol Cybern 73:27–35
47. Sternad D, Turvey MT, Saltzman EL (1999) Dynamics of 1:2 Coordination: Generalizing Relative Phase to n:m Rhythms. J Mot Behav 31:207–233
48. Kelso JAS, DeGuzman GC, (1988) Order in time: How the cooperation between the hands informs the design of the brain. In: Haken H (ed) Neural and Synergetic Computers. Springer, Berlin
49. DeGuzman GC, Kelso JAS (1991) Multifrequency behavioral patterns and the phase attractive circle map. Biol Cybern 64:485–495

Books and Reviews

Fuchs A, Jirsa VK (eds) (2007) Coordination: Neural, Behavioral and Social Dynamics. Springer, Heidelberg
Jirsa VK, Kelso JAS (eds) (2004) Coordination Dynamics: Issues and Trends. Springer, Heidelberg
Kelso JAS (1995) Dynamics Pattern: The Self-Organization of Brain and Behavior. MIT Press, Cambridge
Haken H (1996) Principles of Brain Functioning. Springer, Heidelberg
Tschacher W, Dauwalder JP (eds) (2003) The Dynamical Systems Approach to Cognition: Concepts and Empirical Paradigms Based on Self-Organization, Embodiment and Coordination Dynamics. World Scientific, Singapore

Multi-Granular Computing and Quotient Structure

Ling Zhang[1], Bo Zhang[2]
[1] Artificial Intelligence Institute, Anhui University, Hefei, Anhui, China
[2] Department of Computer Science, State Key Lab of Intelligent Technology and Systems, Tsinghua University, Beijing, China

Article Outline

Glossary

Granularity Granularity is the relative size, scale, level of detail, or depth of penetration that characterizes an object or system.

Multi-granular computing Humans are good at viewing and solving a problem at different grain-sizes (abstraction levels) and translating from one abstraction level to the others easily. This is one of basic characteristics of human intelligence. The aim of multi-granular computing is intended to investigate the granulation problem in human cognition and endow computers with the same capability to make them more efficient in problem solving.

Quotient set Given a universe X and an equivalence relation R on X, define a set $[X] = \{[x]|x \in X\}, [x] = \{y|y \sim x, y \in X\}$. $[X]$ is called a quotient set with respect to R, or simply a quotient set.

Quotient space Given a topologic space (X, T), T is a topology on X and R is an equivalence relation on X. Define a quotient structure on $[X]$ as $[T] = \{u|p^{-1}(u) \in T, u \subset [X]\}$, where $p: X \to [X]$ is a natural projection from X to $[X]$. Construct a topologic space $([X], [T])$. Space $([X], [T])$ is a quotient space corresponding to R. There are authors who keep the neighborhood system structured but remove the axioms of topology [13,14].

Quotient space model The quotient space model is a mathematical model to represent a problem at different grain-sizes by using the concept of quotient space in algebra. In the model a problem (or a system) is described by a triple (X, T, f), with universe (domain) X, structure T and attribute f. If X represents the universe composed of the objects with the finest grain-size, when we view the same universe X at a coarser grain-size, we have a coarse-grained universe denoted by $[X]$. Then we have a new problem space $([X], [T], [f])$, where $[X]$ is the quotient universe of X, $[T]$ the corresponding quotient structure and $[f]$ the quotient attribute. The coarse space $([X], [T], [f])$ is called a quotient space of space (X, T, f). Therefore, a problem with different grain-sizes can be represented by a family of quotient spaces.